doi: 10.15407/ujpe60.06.0561

V.I. GRYTSAY

Bogolyubov Institute for Theoretical Physics, Nat. Acad. of Sci. of Ukraine
(14b, Metrolohichna Str., Kyiv 03680, Ukraine; e-mail: vgrytsay@bitp.kiev.ua)

PACS 05.45.-a, 05.45.Pq, 05.65.+b

LYAPUNOV INDICES AND THE POINCARÉ MAPPING IN A STUDY OF THE STABILITY OF THE KREBS CYCLE

On the basis of a mathematical model, we continue the study of the metabolic Krebs cycle (or the tricarboxylic acid cycle). For the first time, we consider its consistency and stability, which depend on the dissipation of a transmembrane potential formed by the respiratory chain in the plasmatic membrane of a cell. The phase-parametric characteristic of the dynamics of the ATP level depending on a given parameter is constructed. The scenario of formation of multiple autoperiodic and chaotic modes is presented. Poincaré sections and mappings are constructed. The stability of modes and the fractality of the obtained bifurcations are studied. The full spectra of Lyapunov indices, divergences, KS-entropies, horizons of predictability, and Lyapunov dimensionalities of strange attractors are calculated. Some conclusions about the structural-functional connections determining the dependence of the cell respiration cyclicity on the synchronization of the functioning of the tricarboxylic acid cycle and the electron transport chain are presented.

K e y w o r d s: Krebs cycle, metabolic process, self-organization, strange attractor, bifurcation, Feigenbaum scenario.

The most important task of synergetics is the search for the general physical laws explaining the natural regularity of the formation of a life on the Earth. The first descriptive experiment demonstrating the possibility for a cyclic metabolic process to exist was executed by B.P. Belousov in 1951 [1]. With the help of some chemical substances (citric acid, potassium bromate, cerium, *etc.*), he successfully constructed a model of autooscillatory metabolic process involving the Krebs cycle [2]. By this, he showed for the first time that the vital metabolic processes in a cell can be supported due to their self-organization in the autoperiodic mode.

The tricarboxylic acid cycle occupies a particular place in the vital activity of aerobic cells. As a result of the cyclic metabolic process, the acetyl groups formed in the decay of carbohydrates, fats, and proteins are oxidized there to carbon dioxide. Hydrogen atoms released in this case are transferred into the respiratory chain, where the main source of the energy for a cell, ATP, is produced in the course of the reaction of oxidative phosphorylation. With the help of NADH, there arise the negative feedbacks, due to which the synchronization of the process of catabolism and the respiration of a cell occurs. The joint existence of these metabolic processes is possible only under their self-organization in a single cycle. In addition, the Krebs cycle is a source of molecules-precursors, which are used in the synthesis of compounds important for the vital activity of cells in other biochemical reactions.

Studying the functioning of the tricarboxylic acid cycle was carried out in experiments and theoretically [3–11]. In particular, the given process was analyzed on the basis of the mathematical model of growth of *Candida utilis* cells on ethanol. This model was developed by Professor V.P. Gachok [12, 13]. The analogous approaches to the modeling of a growth

of cells were considered by J. Monod, V.S. Podgorskii, L.N. Drozdov-Tikhomirov, N.T. Rakhimova, G.Yu. Riznichenko, and others [14–18]. Within such models, the unstable modes in the cultivation of cells, which were observed in experiments, were studied. The results of computational experiments concerning the chaotic dynamics described well the experimental characteristics [19].

Then the Gachok model was improved in [20, 21], where the influence of the concentration of CO_2 on the cell respiration intensity and the cyclicity of a respiratory process was taken into account. The structural-functional connections of the metabolic process running in a cell, according to which the appearance of complicated oscillations in the metabolic process in a cell becomes possible, were found. It was concluded that those oscillations arise at the level of redox reactions of the Krebs cycle, reflect the cyclicity of the process, and characterize the self-organization inside a cell. For some modes, the fractality of bifurcations was studied, and the indicators characterizing the stability of strange attractors were established.

Analogous oscillatory modes in the processes of photosynthesis and glycolysis, variations in the concentration of calcium in a cell, and oscillations in a heart muscle and in some biochemical processes were found in [22–26].

The distinction of the present work from other ones consists in the modeling of such significant phenomenon as the influence of the dissipation of a proton potential on the Krebs cycle. By the Mitchell chemoosmotic hypothesis [27], the transmembrane potential arises under the reducing equivalent transfer along the respiratory chain on internal mitochondrial membranes. Then the transport of ions H^+ inward a membrane occurs under the action of the formed electrochemical gradient of the potential. This results in the production of a free energy, whose significant part is stored in ATP. A part of this energy is used also for other purposes, namely: transport of phosphate, transport of ions Ca^{2+}, transformation of ADP to ATP, generation of heat, operation of the "proton-driven turbine" of bacterial flagella, *etc.* The transfer of ions H^+ through F_0F_1-ATPase molecules changes the given potential, which affects the tricarboxylic acid cycle. An analogous process is running in the plasmatic membrane of aerobic cells *Candida utilis* considered in the present work. Thus, the Krebs cycle and the respiratory chain are functioning under a permanent self-organization between each other and depend on the intensity of a dissipation of the electrochemical gradient of the potential in metabolic processes.

We will study the structural-functional connections, according to which the Krebs cycle and the respiratory chain are self-organized and operate as a single complex providing a cell with the necessary energy store for its life. The limits of stability of the cycle depending on the dissipation of the proton potential in various processes of the vital activity of a cell are considered as well.

1. Mathematical Model

The general scheme of the process is presented in Fig. 1. According to it with regard for the mass balance, we have constructed the mathematical model given by Eqs. (1)–(19).

$$\frac{dS}{dt} = S_0\frac{K}{K+S+\gamma\psi} - k_1V(E_1)\frac{N}{K_1+N}V(S) - \alpha_1 S, \tag{1}$$

$$\frac{dS_1}{dt} = k_1V(E_1)\frac{N}{K_1+N}V(S) - k_2V(E_2)\frac{N}{K_1+N}V(S_1), \tag{2}$$

$$\frac{dS_2}{dt} = k_2V(E_2)\frac{N}{K_1+N}V(S_1) - k_3V(S_2^2)V(S_3) - k_4V(S_2)V(S_8), \tag{3}$$

$$\frac{dS_3}{dt} = k_4V(S_2)V(S_8) - k_5V(N^2)V(S_3^2) - k_3V(S_2^2)V(S_3), \tag{4}$$

$$\frac{dS_4}{dt} = k_5V(N^2)V(S_3^2) - k_7V(N)V(S_4) - k_8V(N)V(S_4), \tag{5}$$

$$\frac{dS_5}{dt} = k_7V(N)V(S_4) - 2k_9V(L_1-T)V(S_5), \tag{6}$$

$$\frac{dS_6}{dt} = 2k_9V(L_1-T)V(S_5) - k_{10}V(N)\frac{S_6^2}{S_6^2+1+M_1S_8}, \tag{7}$$

$$\frac{dS_7}{dt} = k_{10}V(N)\frac{S_6^2}{S_6^2+1+M_1S_8} - k_{11}V(N)V(S_7) - k_{12}\frac{S_7^2}{S_7^2+1+M_2S_9}V(\psi^2) + k_3V(S_2^2)V(S_3), \tag{8}$$

$$\frac{dS_8}{dt} = k_{11}V(N)V(S_7) - k_4V(S_2)V(S_8) +$$
$$+ k_6V(T^2)\frac{S^2}{S^2+\beta_1}\frac{N_1}{N_1+(S_5+S_7)^2}, \quad (9)$$
$$\frac{dS_9}{dt} = k_{12}\frac{S_7^2}{S_7^2+1+M_2S_9}V(\psi^2) -$$
$$- k_{14}\frac{XTS_9}{(\mu_1+T)[(\mu_2+S_9+X+M_3(1+\mu_3\psi)]S}, \quad (10)$$
$$\frac{dX}{dt} = k_{14}\frac{XTS_9}{(\mu_1+T)[(\mu_2+S_9+X+M_3(1+\mu_3\psi)]S} -$$
$$- \alpha_2X, \quad (11)$$
$$\frac{dQ}{dt} = -k_{15}V(Q)V(L_2-N) +$$
$$+ 4k_{16}V(L_3-Q)V(O_2)\frac{1}{1+\gamma_1\psi^2}, \quad (12)$$
$$\frac{dO_2}{dt} = O_{2_0}\frac{K_2}{K_2+O_2} - k_{16}(L_3-Q)V(O_2)\frac{1}{1+\gamma_1\psi} -$$
$$- k_8V(N)V(S_4) - \alpha_3O_2, \quad (13)$$
$$\frac{dN}{dt} = -k_7V(N)V(S_4) - k_{10}V(N)\frac{S_6^2}{S_6^2+1+M_1S_8} -$$
$$- k_{11}V(N)V(S_7) - k_5V(N^2)V(S_3^2) +$$
$$+ k_{15}V(Q)V(L_2-N) - k_2V(E_2)\frac{N}{K_1+N}V(S_1) -$$
$$- k_1V(E_1)\frac{N}{K_1+N}V(S), \quad (14)$$
$$\frac{dT}{dt} = k_{17}V(L_1-T)V(\psi^2)+k_9V(L-T)V(S_3)-\alpha_4T -$$
$$- k_{18}k_6V(T^2)\frac{S^2}{S^2+\beta_1}\frac{N_1}{N_1+(S_5+S_7)^2} -$$
$$- k_{19}k_{14}\frac{XTS_9}{(\mu_1+T)[\mu_2+S_9+X+M_3(1+\mu_3\psi)S]}, \quad (15)$$
$$\frac{d\psi}{dt} = 4k_{15}V(Q)V(L_2-N)+4k_{17}V((L_1-T)V(\psi^2) -$$
$$- 2k_{12}\frac{S_7^2}{S_7^2+1+M_2S_9}V(\psi^2) - \alpha\psi, \quad (16)$$
$$\frac{dE_1}{dt} = E_{1_0}\frac{S^2}{\beta_2+S^2}\frac{N_2}{N_2+S_1} -$$
$$- n_1V(E_1)\frac{N}{K_1+N}V(S) - \alpha_5E_1, \quad (17)$$
$$\frac{dE_2}{dt} = E_{2_0}\frac{S_1^2}{\beta_3+S_1^2}\frac{N_3}{N_3+S_2} -$$
$$- n_2V(E_2)\frac{N}{K_1+N}V(S_1) - \alpha_6E_2, \quad (18)$$
$$\frac{dC}{dt} = k_8V(N)V(S_4) - \alpha_7C, \quad (19)$$

where $V(X) = X/(1+X)$ is the function that describes the adsorption of the enzyme in the region of a local coupling. The variables of the system are dimensionless [12, 13].

The internal parameters of the system are as follows:

$k_1 = 0.3$; $k_2 = 0.3$; $k_3 = 0.2$; $k_4 = 0.6$;
$k_5 = 0.16$; $k_6 = 0.7$; $k_7 = 0.08$; $k_8 = 0.022$;
$k_9 = 0.1$; $k_{10} = 0.08$; $k_{11} = 0.08$; $k_{12} = 0.1$;
$k_{14} = 0.7$; $k_{15} = 0.27$; $k_{16} = 0.18$;
$k_{17} = 0.14$; $k_{18} = 1$; $k_{19} = 10$; $n_1 = 0.07$;
$n_2 = 0.07$; $L = 2$; $L_1 = 2$; $L_2 = 2.5$; $L_3 = 2$;
$K = 2.5$; $K_1 = 0.35$; $K_2 = 2$; $M_1 = 1$;
$M_2 = 0.35$; $M_3 = 1$; $N_1 = 0.6$; $N_2 = 0.03$;
$N_3 = 0.01$; $\mu_1 = 1.37$; $\mu_2 = 0.3$; $\mu_3 = 0.01$;
$\gamma = 0.7$; $\gamma_1 = 0.7$; $\beta_1 = 0.5$; $\beta_2 = 0.4$;
$\beta_3 = 0.4$; $E_{1_0} = 2$; $E_{2_0} = 2$.

The external parameters determining the flow-type conditions are chosen as

$S_0 = 0.05055$; $O_{2_0} = 0.06$; $\alpha = 0.002$;
$\alpha_1 = 0.02$; $\alpha_2 = 0.004$; $\alpha_3 = 0.01$;
$\alpha_4 = 0.01$; $\alpha_5 = 0.01$; $\alpha_6 = 0.01$; $\alpha_7 = 0.0001$.

The model covers the processes of substrate-enzymatic oxidation of ethanol to acetate, the cycle involving tri- and dicarboxylic acids, glyoxylate cycle, and respiratory chain.

The incoming ethanol S is oxidized by the alcohol dehydrogenase enzyme E_1 to acetaldehyde S_1 (1) and then by the acetal dehydrogenase enzyme E_2 to acetate S_2 (2), (3). The formed acetate can participate in the cell metabolism and can be exchanged with the environment. The model accounts for this situation by the change of acetate by acetyl-CoA. On the first stage of the Krebs cycle due to the citrate synthase reaction, acetyl-CoA jointly with oxalacetate S_8 formed in the Krebs cycle create citrate S_3 (4). Then substances $S_4 - S_8$ are created successively on stages (5)–(9). In the model, the Krebs cycle is represented

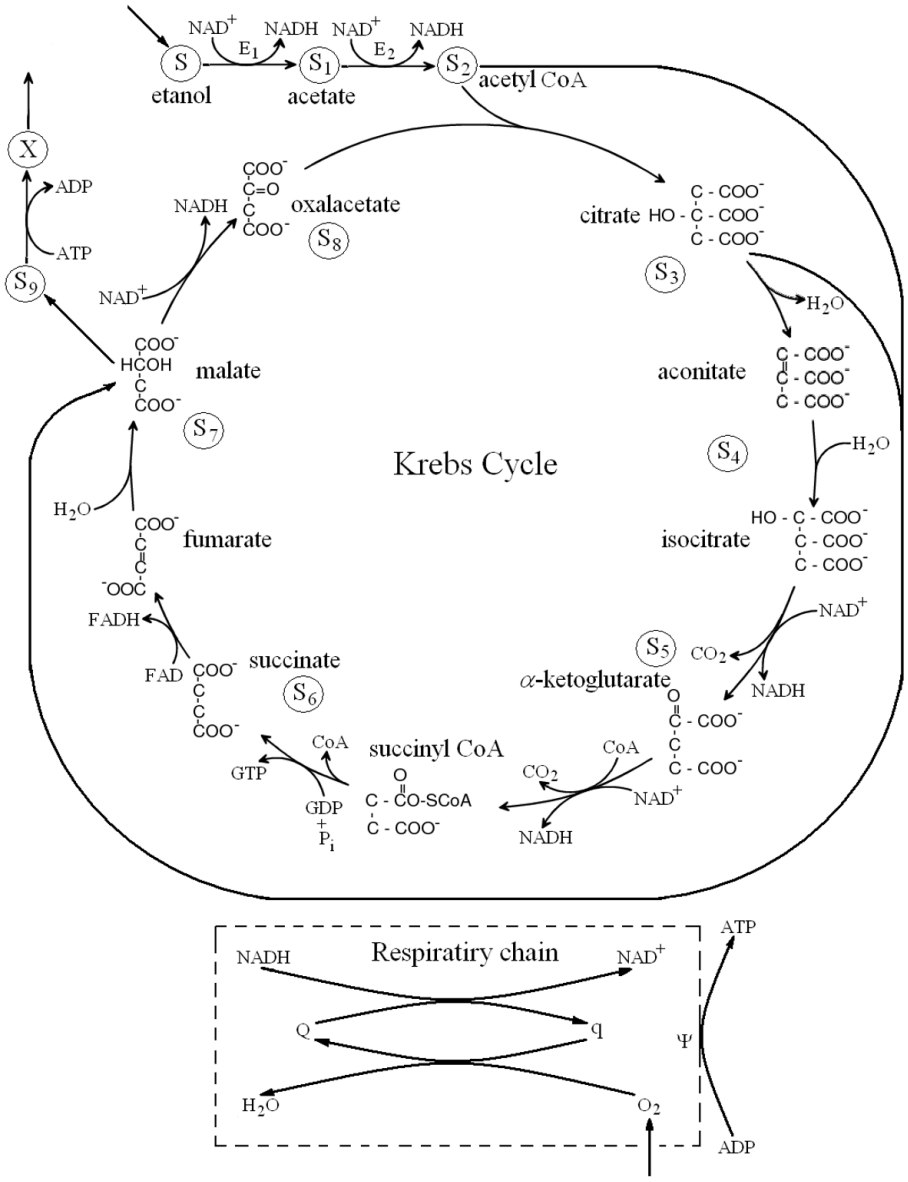

Fig. 1. General scheme of the metabolic process of growth of cells *Candida utilis* on ethanol

by only those substrates that participate in the reduction of NADH and the phosphorylation ADT → ATP. Acetyl-CoA passes along the chain to malate represented in the model as intramitochondrial S_7 (8) and cytosolic S_9 (10) ones. Malate can be also synthesized in another way related to the activity of two enzymes: isocitrate lyase and malate synthetase. The former catalyzes the splitting of isocitrate to succinate, and the latter catalyzes the condensation of acetyl-CoA with glyoxylate and the formation of malate. This glyoxylate-linked way is shown in Fig. 1 as an enzymatic reaction with the consumption of S_2 and S_3 and the formation of S_7. The parameter k_3 controls the activity of the glyoxylate-linked way (3), (4), (8). The yield of S_7 into cytosol is controlled by its concentration, which can increase due to S_9, by causing the inhibition of its transport with the participation of protons of the mitochondrial membrane.

The formed malate S_9 is used by a cell for its growth, namely for the biosynthesis of protein X (11). The energy consumption of the given process is supported by the process ATP $\rightarrow$ ADP. The presence of ethanol in the external solution causes the "ageing" of external membranes of cells, which leads to the inhibition of this process. The inhibition of the process also happens due to the enhanced level of the kinetic membrane potential ψ. The parameter μ_0 is related to the lysis and the washout of cells.

In the model, the respiratory chain of a cell is represented in two forms: oxidized, Q, (12) and reduced, q, ones. They obey the integral of motion $Q(t) + q(t) = L_3$.

A change of the concentration of oxygen in the respiratory chain is determined by Eq. (13).

The activity of the respiratory chain is affected by the level of NADH (14). Its high concentration leads to the enhanced endogenic respiration in the reducing process in the respiratory chain (parameter k_{15}). The accumulation of NADH occurs as a result of the reduction of NAD^+ at the transformation of ethanol and in the Krebs cycle. These variables obey the integral of motion $NAD^+(t) + NADH(t) = L_2$.

In the respiratory chain and the Krebs cycle, the substrate-linked phosphorylation of ADP with the formation of ATP (15) is also realized. The energy consumption due to the process ATP $\rightarrow$ ADP induces the biosynthesis of components of the Krebs cycle (parameter k_{18}) and the growth of cells on the substrate (parameter k_{19}). For these variables, the integral of motion $ATP(t) + ADP(t) = L_1$ holds. Thus, the level of ATP produced in the redox processes in the respiratory chain ADP $\rightarrow$ ATP determines the intensity of the Krebs cycle and the biosynthesis of proteins.

In the respiratory chain, the kinetic membrane potential ψ (16) is created under the running of reducing processes $Q \rightarrow q$. It is consumed at the substrate-linked phosphorylation ADP $\rightarrow$ ATP in the respiratory chain and the Krebs cycle. Its enhanced level inhibits the biosynthesis of proteins and the process of reduction of the respiratory chain.

Equations (17) and (18) describe the activity of enzymes E_1 and E_2, respectively. We consider their biosynthesis (E_{1_0} and E_{2_0}), the inactivation in the course of the enzymatic reaction (n_1 and n_2), and all possible irreversible inactivations (α_5 and α_6).

Equation (19) is related to the formation of carbon dioxide. Its removal from the solution into the environment (α_7) is taken into account. Carbon dioxide is produced in the Krebs cycle (5). In addition, it squeezes out oxygen from the solution (13), by decreasing the activity of the respiratory chain.

The study of solutions of the given mathematical model (1)–(19) was performed with the help of the theory of nonlinear differential equations [28, 29] and the methods of mathematical modeling of biochemical systems applied and developed in [30–47].

To solve this autonomous system of nonlinear differential equations, we applied the Runge—Kutta–Merson method. The accuracy of solutions was set to be 10^{-8}. To get the reliable results, we took the duration of calculations to be 10^6. For this time interval, the system, being in the initial transient state, approaches the asymptotic attractor mode, i.e., its trajectory "sticks" the corresponding attractor.

2. Results of Studies

With the use of the Mitchell hypothesis, we now consider the chain of formation of the proton potential of a cell. For each turnover of the cycle of citric acid, the specific dehydrogenases split off four pairs of hydrogen atoms from isocitrate (5), α-ketoglutarate (6), succinate (7), and malate (8). Their separation into ions H^+ and electrons occurs in the internal membrane through three H^+-transferring loops consisting of ubiquinone and three cytochromes. Each loop transfers two ions H^+ outward the membrane, which leads to the appearance of a transmembrane electrochemical potential (16). The acceptor of electrons in the respiratory chain (12) is oxygen (13). Ions H^+, which are accumulated on the external side of the membrane, move again inward along the electrochemical gradient through molecules of F_0F_1 – ATPase. This transition of ions H^+ from the zone with their high concentration to the zone with a lower one is accompanied by the free energy release. This results in the synthesis of ATP from ADP (15) by the reaction of oxidative phosphorylation. In other words, the continuous turnover of ions H^+ through the membrane occurs. Its driving force is the transfer of electrons along the respiratory chain. Thus, the joint self-organization of the Krebs cycle and the respiratory chain depends on the dynamics of formation of the proton potential. The variation of the potential

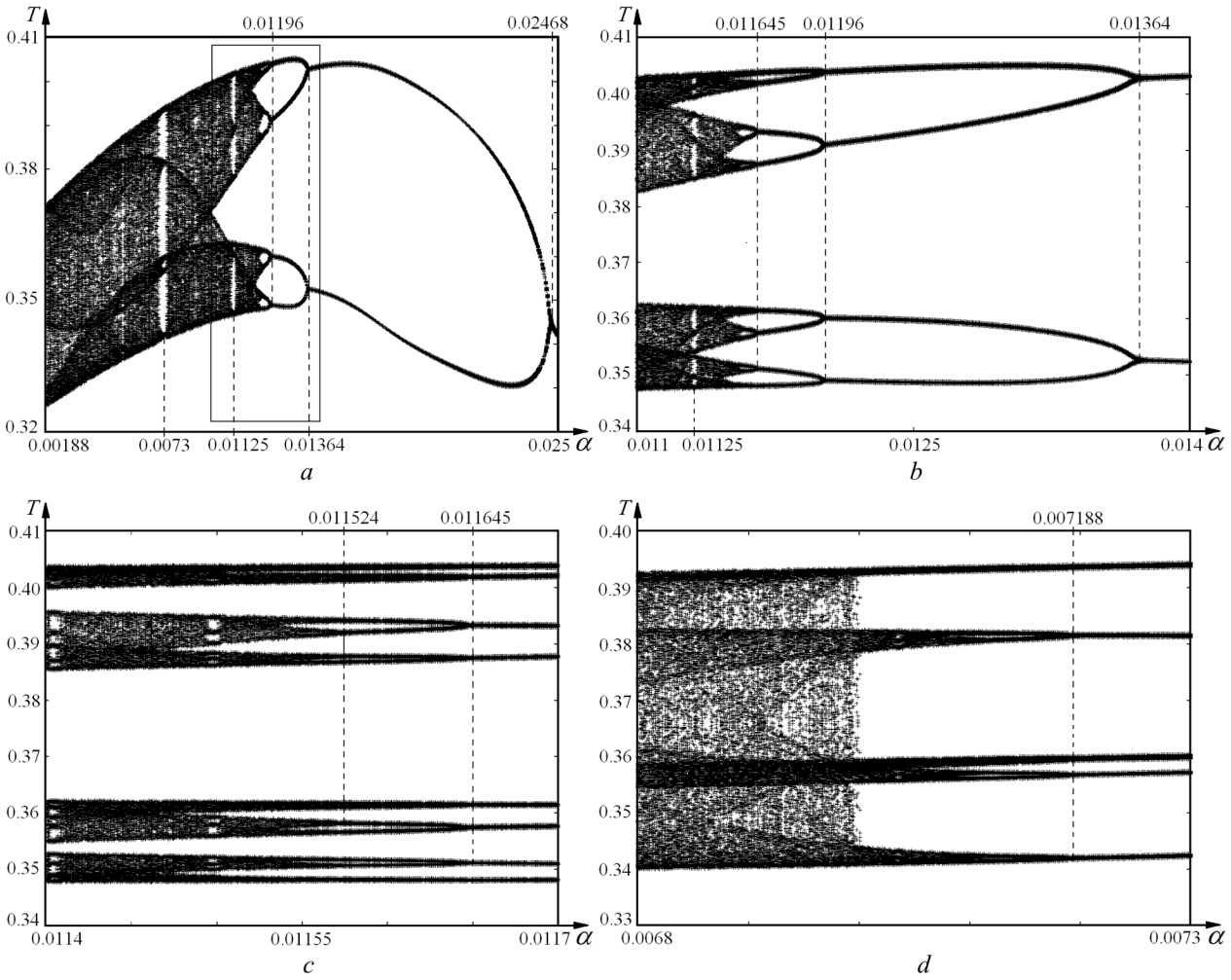

Fig. 2. Phase-parametric diagram for the variable $T(t)$: a – $\alpha \in (0.0018, 0.025)$; b – $\alpha \in (0.011, 0.014)$; c – $\alpha \in (0.0114, 0.0117)$; d – $\alpha \in (0.0068, 0.0073)$

is also affected by its dissipation in other metabolic processes in a cell, besides the current of ions H^+ through the membrane. In the present work, we will study the changes in the dynamics of the Krebs cycle depending on the dissipation of the proton potential.

We now construct the phase-parametric diagram for the multiplicity of autooscillations of the ATP level as a function of the dissipation of the proton potential α (16) (see Fig. 2) by the method of cutting.

In the phase space of a trajectory of the system, we place the cutting plane for $Q = 0.9$. Such choice is explained by the symmetry of oscillations of a level of the oxidized form of the respiratory chain relative to this point in a lot of earlier calculated modes. When the trajectory approaches the attractor, we observe the intersection of the plane by the trajectory in a single direction for every given value of α. On the phase-parametric diagram, we indicate the value of $T(t)$. If a multiple periodic limiting cycle arises, we observe a number of points on the plane, which coincide in the period. If a deterministic chaos appears, the points, where the trajectory intersects the plane, are located chaotically.

Let us consider the diagram in Fig. 2, *a* from right to left. As the value of the coefficient of dissipation α decreases below 0.025, we see the transition from the 1-fold periodic autooscillatory mode to the 2-fold

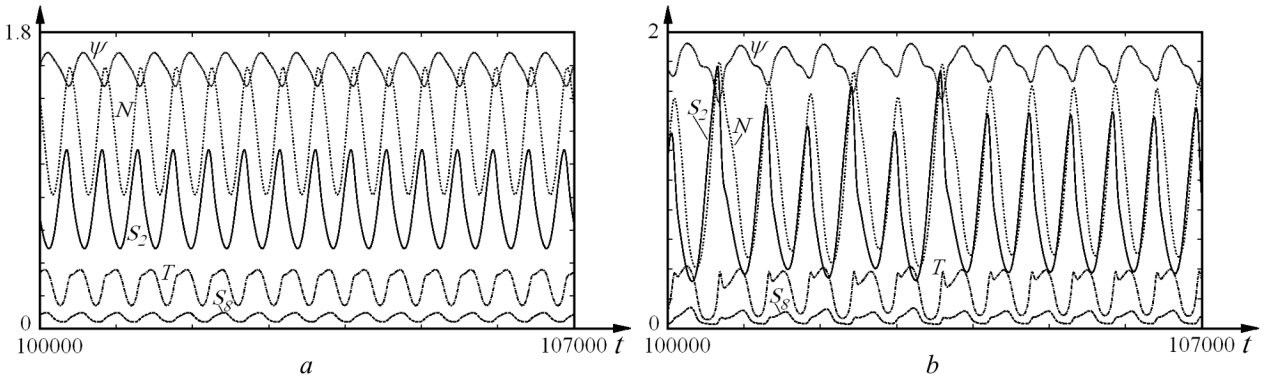

Fig. 3. Kinetic curves of components of the Krebs cycle S_2, S_8, N, ψ, and T: *a* – in the 1-fold periodic mode $1 \cdot 2^0$ for $\alpha = 0.025$; *b* – in the chaotic mode of the strange attractor $1 \cdot 2^x$ for $\alpha = 0.002$

one at the point $\alpha^j = 0.02468$. As a result of the bifurcation, the doubling of the period of oscillations arises. For $\alpha^{j+1} = 0.01364$, we observe the repeated doubling of the period. Then, for $\alpha^{j+2} = 0.01196$, the period of autooscillations is doubled once more.

Let us separate a small section of the diagram for $\alpha \in (0.011, 0.014)$ (Fig. 2, *a*) and represent it in a magnified form (Fig. 2, *b*). For $\alpha^{j+3} = 0.011645$, we see the next bifurcation with the doubling of the period, and the diagram becomes similar to the previous one. The subsequent decrease in the scale of the diagram in Fig. 2, *c* reveals the next bifurcation with the doubling of the period for $\alpha^{j+4} = 0.011524$, and the self-similarity of the diagram is repeated. This indicates the fractal nature of the obtained cascade of bifurcations. After the critical value of the parameter α determined by the accuracy of computer-based calculations, the deterministic chaos takes place. This means that any appeared fluctuation under given instable modes of the real physical system can induce a chaotic mode. This scenario of the transition to a chaos corresponds to the Feigenbaum scenario [48]. We calculated the value of universal Feigenbaum constant by the data on bifurcations and found that it differs from the classical one. This means that the dynamics of system (1)–(19) cannot be reduced completely to a one-dimensional Feigenbaum mapping.

For $\alpha = 0.0073$ and $\alpha = 0.01125$ (Fig. 2, *a*, *b*), we see the appearance of the windows of periodicity. The deterministic chaos is broken, and the periodic and quasiperiodic modes appear. Analogous windows of periodicity are also observed on bifurcation diagrams on a less scale (see Fig. 2, *c*). As the coefficient of dissipation α continues to decrease, the bifurcations arise in the windows of periodicity, and the chaotic modes are seen again (see Fig. 2, *d*). The self-similarity of the formation of the windows of periodicity on large and small scales indicates once more the fractality of the bifurcation diagram.

In Fig. 3, *a*, *b*, we show the kinetic curves for some components of the metabolic process of cell respiration: in the 1-fold periodic ($\alpha = 0.025$) and chaotic ($\alpha = 0.002$) modes.

In Fig. 3, *a*, we see the harmonic interconnection of the autooscillations of acetyl-CoA (S_2), which is supplied to the cycle of citric acid, and oxalacetate (S_8) closing the cycle. Oscillations of the level of $\mathrm{NAD \cdot H}\,(N)$, which transfers electrons to ubiquinone and cytochromes, occur with the same frequency. These hydrogen-transferring and electron-transferring proteins alternate in a respiratory chain, by forming "three loops" in it. Electrons are transferred to oxygen (acceptor of electrons), and ions H^+ move to the external side of the membrane, by producing the gradient of the potential ψ. This gradient creates the driving force for the return of H^+ inward the membrane through a complex ATP-synthetase system. This results in the creation of new covalent bonds, through which the terminal phosphate groups join ADP with the formation of ATP (T).

Autooscillations arisen in the given metabolic process are regulated by the level of dissipation of the proton potential α. Its decrease leads to the successive doubling of the period of autooscillations and, as follows from calculations, to the appearance of chaotic oscillations (Fig. 3, *b*). The decrease in α means, in particular, a decrease in the current of ions H^+ from

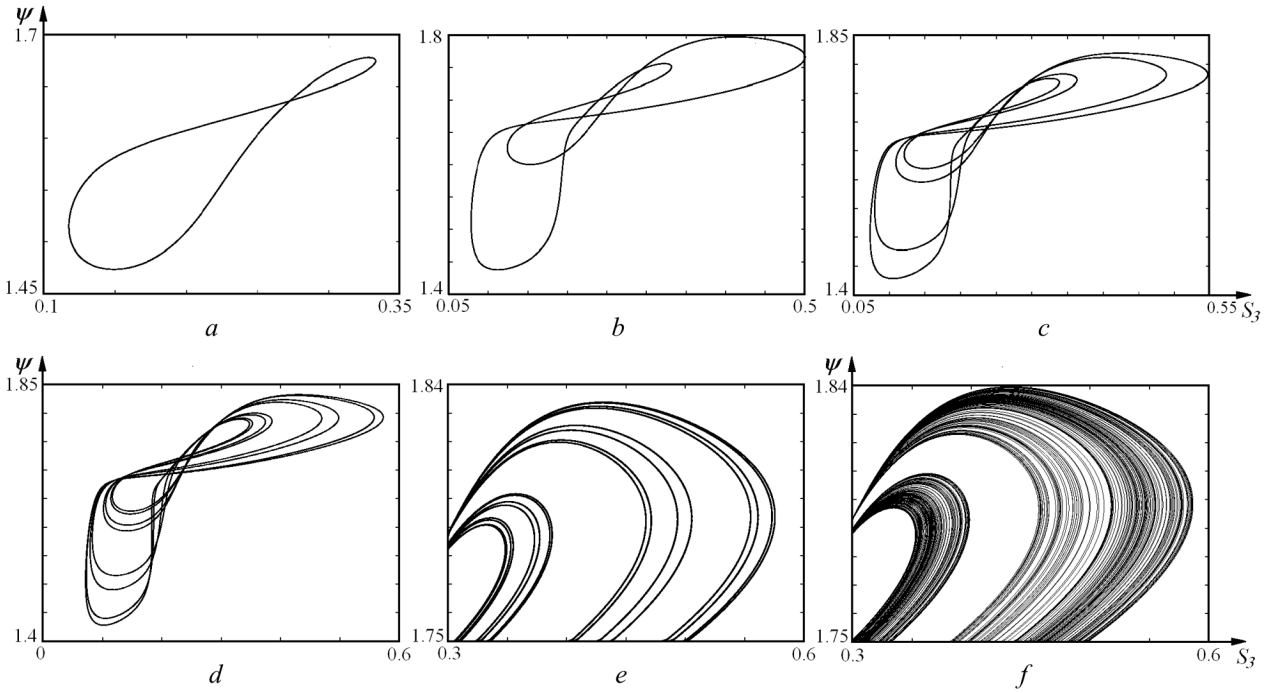

Fig. 4. Projections of system's phase portraits: *a* – regular attractor $1 \cdot 2^0$, $\alpha = 0.025$; *b* – regular attractor $1 \cdot 2^1$, $\alpha = 0.015$; *c* – regular attractor $1 \cdot 2^2$, $\alpha = 0.013$; *d* – regular attractor $1 \cdot 2^3$, $\alpha = 0.0117$; *e* – regular attractor $1 \cdot 2^4$, $\alpha = 0.01158$; *f* – strange attractor $1 \cdot 2^x$, $\alpha = 0.011$

the external side of the membrane to the internal one. The time coordination between the tricarboxylic acid cycle and the transfer of electrons and ions H^+ along the respiratory chain is violated, and the process of oxidative phosphorylation is decelerated. The deceleration of the process of production of ATP increases the rate of the metabolic process involving tricarboxylic acids (7). Moreover, the frequency of the given cycle increases, which causes an increase in the multiplicity of the period of autooscillations. As the parameter α becomes critical, all given metabolic processes become desynchronized, which leads to a chaotic mode (Fig. 3, *b*).

The given sequence demonstrating a growth of the multiplicity of oscillations can be observed in Fig. 4. There, we show the sequential appearance of bifurcations and a complication of the projections of the phase portraits of regular attractors, as the coefficient of dissipation α decreases, until a strange attractor eventually arises (see Fig. 4, *f*). Such scenario can be explained by the existence of positive feedbacks in the given system, which stabilize or intensify the given metabolic processes. For the optimum value of $\alpha = 0.025$, we observe the coordination of the Krebs cycle and the rate of transfer of charges in the respiratory chain. A decrease in α means the deceleration of some metabolic processes related to the dissipation of a membrane potential. The enhanced level of ψ blocks the respiratory chain (12)–(13), by holding it in the reduced state. Under the new conditions, the system reveals the self-organization, by coordinating the dynamics of the tricarboxylic acid cycle with the transfer of electrons along the respiratory chain. In the correspondence with the new appeared cycle, the kinetics of variations in the proton potential gradient and the ATP level are formed.

We now give the example of a possible test of strange attractors for the fractality. Let us consider the strange attractor $1 \cdot 2^x$ (Fig. 5, *a*) formed for $\alpha = 0.0078$. We separate a small rectangular area of the projection of the phase space $t \in (100000, 115000)$ with a single phase curve and represent it in Fig. 5, *b*. The calculation of a phase portrait was executed in the interval $t \in (100000, 320000)$. As is seen, the geometric structure of the given strange attractor is repeated on small and large scales of the projection of

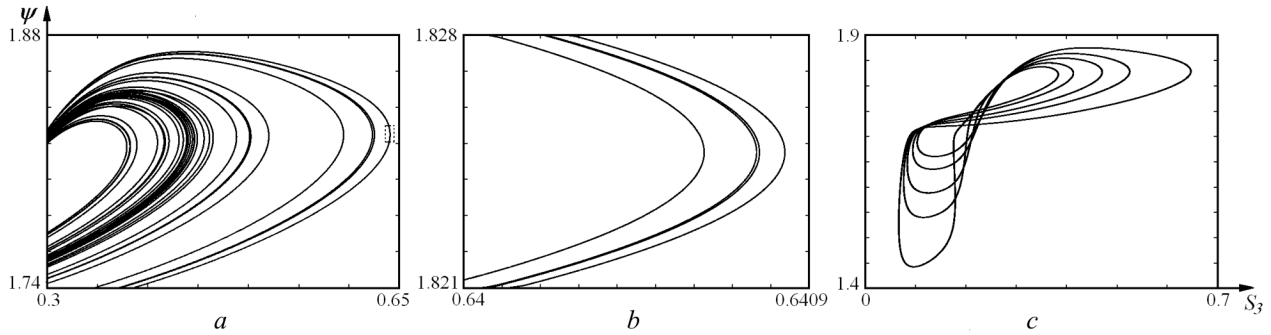

Fig. 5. Projections of system's phase portraits: a – strange attractor $1 \cdot 2^x$, $\alpha = 0.0078$, $t \in (100000, 115000)$; b – strange attractor $1 \cdot 2^x$, $\alpha = 0.0078$ $t \in (100000, 320000)$; c – regular attractor $5 \cdot 2^0$, $\alpha = 0.0073$

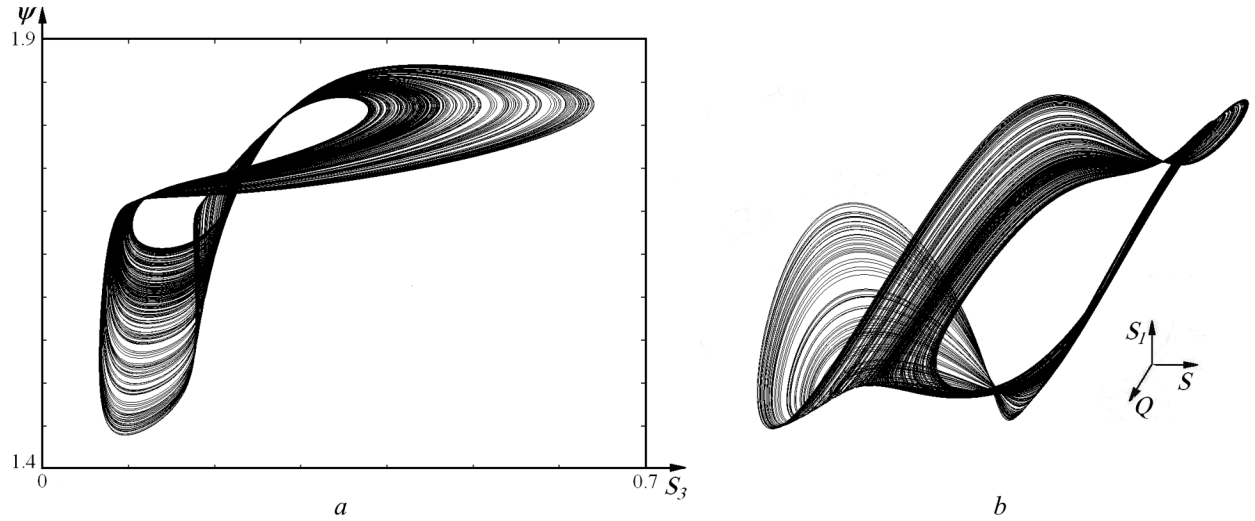

Fig. 6. Projections of the phase portraits of the strange attractor $1 \cdot 2^x$, $\alpha = 0.0078$: a – 2-dimensional projection in the coordinates (S_3, ψ); b – 3-dimensional projection in the coordinates (S, S_1, Q)

the phase portrait. Each appeared curve of the projection of the chaotic attractor is a source of the formation of new curves. Moreover, the geometric regularity of the construction of trajectories in the phase space is repeated. This fact confirms once more that the phase-parametric diagrams are similar on small and large scales, which testifies to the fractal nature of the given strange attractor.

In Fig. 5, c, we present a projection of the phase portrait of the regular attractor $5 \cdot 2^0$ formed in a window of periodicity (Fig. 2) for $\alpha = 0.0073$. The deterministic chaos is destroyed, and the periodic mode is established. The identical windows of periodicity are observed also on smaller scales of the diagram. Outside these windows, the chaotic modes are formed.

As an example, Fig. 6, a, b shows 2- and 3-dimensional projections of the phase portrait of the strange attractor for $\alpha = 0.0078$.

In Fig. 7, a, b, c, we give the constructed projection of a section by the plane $N = 1.128$ and Poincaré maps for the given strange attractor. The choice of a cutting surface was such that the phase trajectory $N(t)$ under a decrease in the given component intersects it the maximally possible number of times, and the tangency is excluded. Figure 7, a indicates the chaoticity of the given strange attractor in the plane (Q, O_2). The Poincaré map for (Q_n, Q_{n+1}) shows the instability of the phase curve for the given component. Points of the map are located randomly on a large part of the area. At the same time, the Poincaré map for $(O_{2_n}, O_{2_{n+1}})$ has a

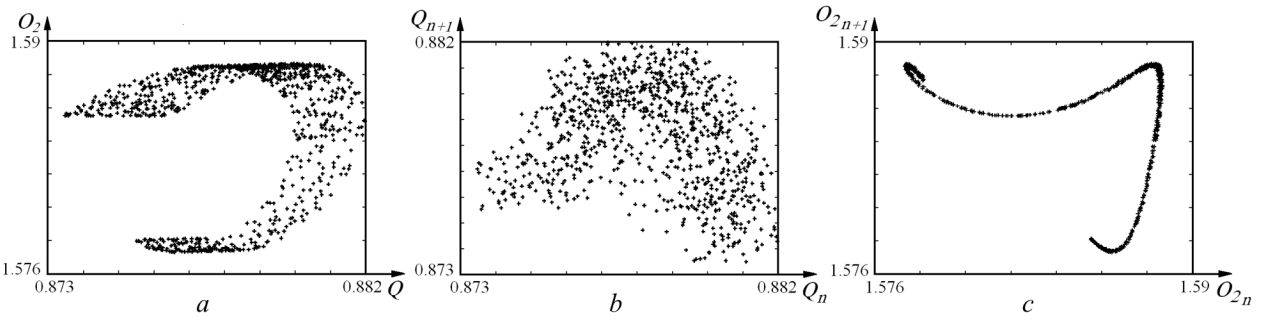

Fig. 7. Projection of the section by the plane $N = 1.128$ (a) and Poincaré maps (b, c) of the strange attractor $1 \cdot 2^x$ for $\alpha = 0.0078$

quasistrip form. The shape of the given curve is independent of the number of points of the mapping. All points of the mapping lie on this curve. The chaos for the given component exists only in the limits of this curve. Along this direction of the phase space, the trajectory of the strange attractor is stable, but aperiodic.

The chaoticity for each component has the own regularity. With the help of Poincaré mappings, it is possible to study the system and to find the reason for the formation of a specific type of the strange attractor of the system. This allows one to investigate the structural-functional connections in the metabolic process and the reasons, for which the appearance of chaotic modes becomes possible.

In order to uniquely identify the type of obtained attractors and to determine their stability, we calculated the full spectra of Lyapunov indices and their sum $\Lambda = \sum_{j=1}^{19} \lambda_j$ for the chosen points. The calculation was carried out by Benettin's algorithm with the orthogonalization of the vectors of perturbations by the Gram–Schmidt method [29].

As a specific feature of calculations of the given indicators, we mention the complexity of the computer-based determination of the perturbation vectors presented by 19×19 matrices.

The algorithm of calculations of the full spectrum of Lyapunov indices consisted in the following. Taking some point on the attractor $\overline{Y_0}$ as the initial one, we traced the trajectory outgoing from it and the evolution of K perturbation vectors. In our case, $K = 19$ (the number of variables of the system). The initial equations of the system supplemented by 19 complexes of equations in variations were solved numerically. As the initial perturbation vectors, we set the collection of vectors $\overline{b_1^0}, \overline{b_2^0}, ..., \overline{b_{19}^0}$, which are mutually orthogonal and normed by one. In some time Δt, the trajectory arrives at a point $\overline{Y_1}$, and the perturbation vectors become $\overline{b_1^1}, \overline{b_2^1}, ..., \overline{b_{19}^1}$. Their renormalization and orthogonalization by the Gram–Schmidt method are performed by the following scheme:

$$\overline{b_1^1} = \frac{\overline{b_1}}{\left\|\overline{b_1}\right\|},$$

$$\overline{b_2'} = \overline{b_2^0} - (\overline{b_2^0}, \overline{b_1^1})\overline{b_1^1}, \quad \overline{b_2^1} = \frac{\overline{b_2'}}{\left\|\overline{b_2'}\right\|},$$

$$\overline{b_3'} = \overline{b_3^0} - (\overline{b_3^0}, \overline{b_1^1})\overline{b_1^1} - (\overline{b_3^0}, \overline{b_2^1})\overline{b_2^1}, \quad \overline{b_3^1} = \frac{\overline{b_3'}}{\|b_3'\|},$$

$$\overline{b_4'} = \overline{b_4^0} - (\overline{b_4^0}, \overline{b_1^1})\overline{b_1^1} - (\overline{b_4^0}, \overline{b_2^1})\overline{b_2^1} - (\overline{b_4}, \overline{b_3^1})b_3^1, \quad \overline{b_4^1} = \frac{\overline{b_4'}}{\|b_4'\|},$$

.....

$$\overline{b_{19}'} = \overline{b_{19}^0} - (\overline{b_{19}^0}, \overline{b_1^1})\overline{b_1^1} - (\overline{b_{19}^0}, \overline{b_2^1})\overline{b_2^1} - (\overline{b_{19}}, \overline{b_3^1})b_3^1 - ... -$$

$$-(\overline{b_{19}}, \overline{b_{18}^1})b_{18}^1, \quad \overline{b_{19}^1} = \frac{\overline{b_{19}'}}{\|b_{19}'\|},$$

Then the calculations are continued, by starting from the point $\overline{Y_1}$ and perturbation vectors $\overline{b_1^1}, \overline{b_2^1}, ..., \overline{b_{19}^1}$. After the next time interval Δt, a new collection of perturbation vectors $\overline{b_1^2}, \overline{b_2^2}, ..., \overline{b_{19}^2}$ is formed and undergoes again the orthogonalization and the renormalization by the above-indicated scheme. The described sequence of manipulations is repeated a sufficiently large number of times, M. In this case in the course of calculations, we evaluated the sums

$$Z_1 = \sum_{i=1}^{M} \ln \left\|b_1'^i\right\|,$$

$$Z_2 = \sum_{i=1}^{M} \ln \|b_2'\|,$$

.....,

$$Z_{19} = \sum_{i=1}^{M} \ln \|b_{19}'^{i}\|$$

which involve the perturbation vectors prior to the renormalization, but after the normalization.

The estimation of 19 Lyapunov indices was carried out in the following way:

$$\lambda_j = \frac{Z_j}{MT}, \quad j = 1, 2, ..., 19.$$

Below for the sake of comparison, we present the spectra of Lyapunov indices for some modes of the system. For brevity without any loss of information, we give the values of indices up to the fourth decimal point.

The ratios of the values of Lyapunov indices $\lambda_1 > > \lambda_2 > \lambda_3 > ... > \lambda_{19}$ serve as the criterion of the validity of calculations. For a regular attractor, we have obligatorily $\lambda_1 - \lambda_{19}$. The remaining indices can be also ≈ 0 in some cases. In some other cases, they are negative. The zero value of the first Lyapunov index testifies to the presence of a stable limiting cycle.

For a strange attractor, at least one Lyapunov index must be positive. After it, the zero index follows. The next indices are negative. The presence of negative indices means the contraction of system's phase space in the corresponding directions, whereas the positive indices indicate the dispersion of trajectories. Therefore, there occurs the mixing of trajectories in narrow places of the phase space of the system, i.e., there appears the deterministic chaos. The Lyapunov indices contain obligatorily the zero index, which means the conservation of the aperiodic trajectory of an attractor in some region of the phase space and the existence of a strange attractor.

For $\alpha = 0.025$, the regular attractor $1 \cdot 2^0$ arises. We have $\lambda_1 - \lambda_{19}$: .0000, –.0001, –.0002, –.0040, –.0147, –.0230, –.0241, –.0254, –.0355, –.0355, –.0355, –.0355, –.0362, –.0369, –.0897, –.1091, –.1090, –.1221, –.1507. $\Lambda = -.8872$.

For $\alpha = 0.015$ – regular attractor $1 \cdot 2^1$; $\lambda_1 - \lambda_{19}$: .0000, –.0002, –.0006, –.0040, –.0135, –.0193, –.0232, –.0284, –.0316, –.0322 –.0322, –.0322, –.0406, –.0436, –.0849, –.1000, –.1000, –.1192, –.1530. $\Lambda = -.8586$.

For $\alpha = 0.013$ – regular attractor $1 \cdot 2^2$; $\lambda_1 - \lambda_{19}$: .0000, –.0002, –.0008, –.0040, –.0127, –.0194, –.0237, –.0297, –.0304, –.0320, –.0320, –.0320, –.0409, –.0432, –.0845, –.0981, –.0981, –.1183, –.1531. $\Lambda = -.8531$.

For $\alpha = 0.0117$ – regular attractor $1 \cdot 2^3$; $\lambda_1 - \lambda_{19}$: .0000, –.0001, –.0002, –.0040, –.0130, –.0194, –.0232, –.0295, –.0306, –.0322, –.0322, –.0322, –.0406, –.0448, –.0834, –.0969, –.0969, –.1179, –.1533. $\Lambda = -.8503$.

For $\alpha = 0.01158$ – regular attractor $1 \cdot 2^4$; $\lambda_1 - \lambda_{19}$: .0000, .0000, –.0002, –.0040, –.0130, –.0194, –.0231, –.0297, –.0305, –.0322, –.0322, –.0322, –.0406, –.0443, –.0840, –.0968, –.0967, –.1178, –.1532. $\Lambda = -.8500$.

For $\alpha = 0.01153$ – strange attractor $1 \cdot 2^x$; $\lambda_1 - \lambda_{19}$: .0001, .0000, –.0002, –.0040, –.0131, –.0194, –.0231, –.0298, –.0305, –.0322, –.0322, –.0322, –.0407, –.0443, –.0840, –.0967, –.0967, –.1178, –.1530. $\Lambda = -.8496$.

For $\alpha = 0.011$ – strange attractor $1 \cdot 2^x$; $\lambda_1 - \lambda_{19}$: .0003, .0000, –.0002, –.0040, –.0132, –.0193, –.0228, –.0305, –.0306, –.0317, –.0317, –.0317, –.0404, –.0443, –.0842, –.0962, –.0961, –.1176, –.1529. $\Lambda = -.8471$.

For $\alpha = 0.0078$ – strange attractor $1 \cdot 2^x$; $\lambda_1 - \lambda_{19}$: .0007, .0000, –.0002, –.0040, –.0129, –.0200, –.0213, –.0297, –.0311, –.0326, –.0326, –.0326, –.0415, –.0449, –.0831, –.0928, –.0928, –.1164, –.1527. $\Lambda = -.8401$.

For $\alpha = 0.00735260$, we have the transition between the strange attractors $1 \cdot 2^x \leftrightarrow 5 \cdot 2^x$. $\lambda_1 - \lambda_{19}$: .0003, .0000, –.0002, –.0040, –.0125, –.0200, –.0210, –.0296, –.0309, –.0322, –.0322, –.0322, –.0406, –.0459, –.0829, –.0926, –.0926, –.1168, –.1532. $\Lambda = -.8390$.

For $\alpha = 0.00735255$ – strange attractor $5 \cdot 2^x$; $\lambda_1 - \lambda_{19}$: .0003, .0000, –.0002, –.0040, –.0125, –.0200, –.0210, –.0296, –.0310, –.0321, –.0321, –.0321, –.0405, –.0459, –.0829, –.0926, –.0926, –.1170, –.1534. $\Lambda = -.8392$.

For $\alpha = 0.0073$ – regular attractor $5 \cdot 2^0$; $\lambda_1 - \lambda_{19}$: .0000, –.0002, –.0008, –.0039, –.0118, –.0200, –.0209, –.0296, –.0308, –.0321, –.0321, –.0321, –.0405, –.0460, –.0828, –.0926, –.0926, –.1171, –.1533. $\Lambda = -.8390$.

For $\alpha = 0.00715$ – regular attractor $5 \cdot 2^1$; $\lambda_1 - \lambda_{19}$: .0000, –.0001, –.0004, –.0047, –.0113, –.0201, –.0209, –.0297, –.0307, –.0322, –.0322, –.0322, –.0405, –.0460, –.0827, –.0925, –.0924, –.1171, –.1533. $\Lambda = -.8389$.

For $\alpha = 0.0071$ – regular attractor $5 \cdot 2^2$; $\lambda_1 - \lambda_{19}$: .0000, –.0001 –.0002, –.0040, –.0123, –.0201, –.0208, –.0297, –.0307, –.0322, –.0322, –.0322, –.0405, –.0461, –.0826, –.0924, –.0924, –.1171, –.1533. $\Lambda = -.8388$.

For $\alpha = 0.0070$ – strange attractor $5 \cdot 2^x$; $\lambda_1 - \lambda_{19}$: .0004, .0000, –.0002, –.0041, –.0126, –.0200, –.0208, –.0297, –.0306, –.0325, –.0325, –.0325, –.0406, –.0462, –.0826, –.0922, –.0922, –.1168, –.1533. $\Lambda = -.8388$.

For $\alpha = 0.00695$, we have the transition between the strange attractors $5 \cdot 2^x \leftrightarrow 1 \cdot 2^x$. $\lambda_1 - -\lambda_{19}$: .0006, .0000, –.0002, –.0040, –.0127, –.0199, –.0209, –.0298, –.0306, –.0326, –.0326, –.0326, –.0407, –.0462, –.0827, –.0921, –.0920, –.1165, –.1530. $\Lambda = -.8385$.

For $\alpha = 0.002$ – strange attractor $1 \cdot 2^x$; $\lambda_1 - \lambda_{19}$: .0007, .0000, –.0002, –.0040, –.0122, –.0190, –.0205, –.0290, –.0308, –.0324, –.0324, –.0324, –.0410, –.0477, –.0812, –.0871, –.0870, –.1167, –.1528. $\Lambda = -.8256$.

These calculations allow us to uniquely identify the type of attractors in the corresponding modes. A decrease in the coefficient of dissipation of the transmembrane potential causes sequential bifurcations in the 1-fold periodic mode $1 \cdot 2^0 \rightarrow 1 \cdot 2^n$, until the modes of the strange attractors $1 \cdot 2^x$ arise eventually. We observe the "order-chaos" transition. As the dissipation decreases further, the windows of periodicity appear. In them, the 5-fold periodic modes $5 \cdot 2^0 \rightarrow 5 \cdot 2^n$ are formed. As a result of sequential bifurcations, the strange attractors $5 \cdot 2^x$ arise. We observe also the "chaos-chaos" transitions: $1 \cdot 2^x \leftrightarrow 5 \cdot 2^x$ and $5 \cdot 2^x \leftrightarrow 1 \cdot 2^x$. Thus, the metabolic system has possibilities for the self-organization and the adaptation to varying conditions.

By the given Lyapunov indices for strange attractors, we determine the KS-entropy (the Kolmogorov–Sinai entropy) [49]. By the Pesin theorem [50], the KS-entropy $h$corresponds to the sum of all positive Lyapunov characteristic indices.

The KS-entropy allows us to judge the rate, with which the information about the initial state of the system is lost. The positivity of the given entropy is a criterion of the chaos. This gives possibility to qualitatively estimate the properties of attractor's local stability.

We determine also the quantity inverse to the KS-entropy, $t_{\min}$. This is the time of a mixing in the system. It characterizes the rate, with which the initial conditions will be forgotten. For $t \ll t_{\min}$, the behavior of the system can be predicted with sufficient accuracy. For $t > t_{\min}$, only a probabilistic description is possible. The chaotic mode is not predictable due to the loss of the memory of initial conditions. The quantity $t_{\min}$ is called the Lyapunov index and characterizes the "horizon of predictability" of a strange attractor.

In order to classify the geometric structure of strange attractors, we calculated the dimension of their fractality. The strange attractors are fractal sets and have the fractional Hausdorff–Besicovitch dimension. But its direct calculation is a very labor-consuming task possessing no standard algorithm. Therefore, as a quantitative measure of the fractality, we calculated the Lyapunov dimension of attractors by the Kaplan–Yorke formula [51, 52]:

$$D_{F_r} = m + \frac{\sum\limits_{j=1}^{m} \lambda_j}{|\lambda_{m+1}|},$$

where m is the number of the first Lyapunov indices ordered by their decreasing. Their sum $\sum_{j=1}^{m} \lambda_j \geqslant 0$, and $m+1$ is the number of the first Lyapunov index, whose value $\lambda_{m+1} < 0$.

For the above-considered strange attractors, we obtained the following indices.

$1 \cdot 2^x$ ($\alpha = 0.01153$): $h = 0.0001$, $t_{\min} = 10000$, $D_{F_r} = 2.5$;

$1 \cdot 2^x$ ($\alpha = 0.011$): $h = 0.0003$, $t_{\min} = 3333.3$, $D_{F_r} = 3.5$;

$1 \cdot 2^x$ ($\alpha = 0.078$): $h = 0.0007$, $t_{\min} = 1428.6$, $D_{F_r} = 5.5$;

$1 \cdot 2^x \leftrightarrow 5 \cdot 2^x$ ($\alpha = 0.00735260$): $h = 0.0003$, $t_{\min} = 3333.3$, $D_{F_r} = 3.5$;

$5 \cdot 2^x$ ($\alpha = 0.00735255$): $h = 0.0003$, $t_{\min} = 3333.3$, $D_{F_r} = 3.5$;

$5 \cdot 2^x$ ($\alpha = 0.0070$): $h = 0.0004$, $t_{\min} = 2500$, $D_{F_r} = 5.0$;

$5 \cdot 2^x \leftrightarrow 1 \cdot 2^x$ ($\alpha = 0.00695$): $h = 0.0006$, $t_{\min} = 1666.7$, $D_{F_r} = 6$.

$1 \cdot 2^x$ ($\alpha = 0.002$): $h = 0.0007$, $t_{\min} = 1428.6$, $D_{F_r} = 5.5$.

By the values of calculated indicators, we may judge the distinction of the structures of the given strange attractors. The higher the Lyapunov dimensionality, the more pronounced the chaoticity of an attractor in the phase space. As the Lyapunov dimensionality decreases, the phase curves approach one another in an element of the phase space (cf. the Lyapunov dimensionalities and the chaoticity of strange attractors in Fig. 4, *f* and Fig. 6, *a*). Starting from the structure of a strange attractor, we can conclude about the degree of stability of various modes and about the adaptation of the metabolic process in a cell to external influences.

3. Conclusions

With the help of the mathematical model, we have studied the self-organization of the Krebs cycle and the respiratory chain of a cell depending on the dissipation of the transmembrane potential. The work is based on the Mitchell hypothesis about the formation of a transmembrane potential and its dissipation under phosphorylation and its consumption in other metabolic processes. The bifurcation diagram is constructed, and a scenario of variation of the multiplicity of the autooscillatory metabolic process is found. As the dissipation decreases, the multiplicity of the cycle is doubled by the Feigenbaum scenario, until the aperiodic modes of strange attractors arise eventually. They are transformed in stable periodic modes as a result of the self-organization. This means that the metabolic process is adapted to varying conditions. The Poincaré sections and maps for attractors are constructed. The full spectra of Lyapunov indices and the divergences for various modes are calculated. For some strange attractors, we have calculated the KS-entropies, "horizons of predictability," and the Lyapunov dimensionalities of attractors. The obtained results allow one to study the structural-functional connections, by which the transmembrane potential affects the dynamics of the Krebs cycle and the respiratory chain, and to study the physical laws of a self-organization in the metabolic process in cells.

The work is supported by the project No. 0113U001093 of the National Academy of Sciences of Ukraine.

1. B.P. Belousov, in: *Autowave Processes in Systems with Diffusion* (Gor'kii State Univ., Gor'kii, 1951), p. 76 (in Russian).
2. H.A. Krebs and W.A. Johnson, Enzymologia, No. 4, 148 (1937).
3. R. Bohnensack and E.E. Sel'kov, Studia biophys. **66**, 47 (1977).
4. A.E. Lyubarev and B.I. Kurganov, Molekul. Biol. **21**, 1286 (1987).
5. E.M.T. El-Mansi, G.C. Dawson, and C.F.A. Bryce, Comput. Appl. Biosci. **10**, 295 (1994).
6. R. Ramakrishna, J.S. Edwards, A. McCulloch, and B.O. Palsson, Am. J. Physiol. Regul. Integr. Comp. Physiol. **280**, R695 (2001).
7. S. Cortassa, M.A. Aon, E. Marban, R.L. Winslow, and B. O'Rourke, Biophys. J. **84**, 2734 (2003).
8. K. Yugi and M. Tomita, Bioinform. **20**, 1795 (2004).
9. V.K. Singh and I. Ghosh, Theor. Biol. Med. Model. **3**, 27 (2006).
10. E. Mogilevskaya, O. Demin, and I. Goryanin, J. of Biol. Phys. **32**(3-4), 245 (2006).
11. D.L. Nelson and M.M. Cox, *Lehninger Principles of Biochemistry* (Freeman, New York, 2008).
12. V.P. Gachok, *Kinetics of Biochemical Processes* (Naukova Dumka, Kiev, 1988) (in Russian).
13. V.P. Gachok, *Strange Attractors in Biosystems* (Naukova Dumka, Kiev, 1989) (in Russian).
14. J. Monod, *Recherches sur la Croissanse des Cultures Bacteriennes* (Hermann, Paris, 1942).
15. V.S. Podgorskii, *Physiology and Metabolism of Methanol-Consuming Yeast* (Naukova Dumka, Kiev, 1982) (in Russian).
16. L.N. Drozdov-Tikhomirov and N.T. Rakhimova, Mikrobiol. **55**, 775 (1986).
17. G.Yu. Riznichenko, *Mathematical Models in Biophysics and Ecology* (Inst. of Computer Studies, Moscow–Izhevsk, 2003) (in Russian).
18. C.M. Watteeuw, W.B. Armiger, D.L. Ristroph, and A.E. Humphrey, Biotechnol. Bioeng. **21**, 1221 (1979).
19. W.B. Armiger, A.R. Moreira, J.A. Phillips, and A.E. Humphrey, in: *Utilization of Cellulose Materials in Inconventional Food Production* (Plenum, New York, 1979), p. 111.
20. V.I. Grytsay and I.V. Musatenko, Ukr. Biokhim. Zh. **85**, 191 (2013).
21. V. Grytsay and I. Musatenko, in: *Chaotic Modeling and Simulation (CMSIM)* (2014), Vol. 3, p. 207.
22. E.E. Selkov, Europ. J. Biochem. **4**, 79 (1968).
23. B. Hess and A. Boiteux, Annu. Rev. Biochem. **40**, 237 (1971).
24. A. Goldbeter and R. Lefer, Biophys. J. **12**, 1302 (1972).
25. A. Godlbeter and R. Caplan, Annu. Rev. Biophys. Bioeng. **5**, 449 (1976).
26. *Chaos in Chemical and Biochemical Systems*, edited by R. Field and L. Györgyi (World Scientific, Singapore, 1993).
27. P. Mitchell, FEBS Lett. **43**, 189 (1974).
28. V.S. Anishchenko, *Complex Oscillations in Simple Systems*(Nauka, Moscow, 1990) (in Russian).
29. S.P. Kuznetsov, *Dynamical Chaos* (Fiz.-Mat. Nauka, Moscow, 2001) (in Russian).
30. V.P. Gachok and V.I. Grytsay, Dokl. Akad. Nauk SSSR **282**, 51 (1985).
31. V.P. Gachok, V.I. Grytsay, A.Yu. Arinbasarova, A.G. Medentsev, K.A. Koshcheyenko, and V.K. Akimenko, Biotechn. Bioengin. **33**, 661 (1989).
32. V.P. Gachok, V.I. Grytsay, A.Yu. Arinbasarova, A.G. Medentsev, K.A. Koshcheyenko, and V.K. Akimenko, Biotechn. Bioengin. **33**, 668 (1989).
33. V.I. Grytsay, Dopov. Nats. Akad. Nauk Ukr., No. 2, 175 (2000).
34. V.I. Grytsay, Dopov. Nats. Akad. Nauk Ukr., No. 3, 201 (2000).
35. V.I. Grytsay, Dopov. Nats. Akad. Nauk Ukr., No. 11, 112 (2000).

36. V.I. Grytsay, Ukr. J. Phys. **46**, 124 (2001).
37. V.V. Andreev and V.I. Grytsay, Matem. Modelir. **17**, No. 2, 57 (2005).
38. V.V. Andreev and V.I. Grytsay, Matem. Modelir. **17**, No. 6, 3 (2005).
39. V.I. Grytsay and V.V. Andreev, Matem. Modelir. **18**, No. 12, 88 (2006).
40. V.I. Grytsay, Medium. Romanian J. Biophys. **17**, 55 (2007).
41. V.I. Grytsay, Biofiz. Visn., No. 2, 92 (2007).
42. V.I. Grytsay, Biofiz. Visn., No. 2, 25 (2008).
43. V.I. Grytsay, Ukr. J. Phys. **55**, 599 (2010).
44. V.I. Grytsay and I.V. Musatenko, Ukr. Biochem. J. **85**, 93 (2013).
45. V.I. Grytsay and I.V. Musatenko, Ukr. J. Phys. **58**, 677 (2013).
46. V.I. Grytsay and I.V. Musatenko, in: *Self-Organization and Chaos, Chaotic Modeling and Simulation (CMSIM)*, No. 4, 539 (2013).
47. V.I. Grytsay and I.V. Musatenko, Biopolym. Cell **30**, 404 (2014).
48. M.J. Feigenbaum, J. Stat. Phys. **19**, 25 (1978).
49. A.N. Kolmogorov, Dokl. Akad. Nauk SSSR **154**, 754 (1959).
50. Ya.B. Pesin, Usp. Mat. Nauk. **32**, No. 4, 55 (1977).
51. J.L. Kaplan and J.A. Yorke, Ann. N. Y. Acad. Sci. **316**, 400 (1979).
52. J.L. Kaplan and J.A. Yorke, in: *Functional Differential Equations of Fixed Points*, edited by H.O. Peitgen, H.O. Walther (Springer, Berlin, 1979), Vol. 730, p. 204.

Received 14.04.15

В.Й. Грицай

ПОКАЗНИКИ ЛЯПУНОВА
ТА ВІДОБРАЖЕННЯ ПУАНКАРЕ
В ДОСЛІДЖЕННІ СТІЙКОСТІ ЦИКЛУ КРЕБСА

Р е з ю м е

В даній роботі за допомогою математичної моделі продовжується дослідження метаболічного процесу циклу Кребса. Вперше досліджується узгодженість та стійкість циклу трикарбонових кислот в залежності від дисипації трансмембранного потенціалу, утвореного дихальним ланцюгом в плазматичній мембрані клітини. Побудована фазопараметрична характеристика залежності динаміки зміни рівня АТФ від величини даного параметра. Знайдено сценарій формування багатократних автоперіодичних та хаотичних режимів. Побудовано Пуанкаре перерізи та відображення. Досліджено стійкість режимів та фрактальність знайдених біфуркацій. Розраховані повні спектри показників Ляпунова, дивергенції, КС-ентропії, горизонти передбачуваності та ляпуновські розмірності дивних атракторів. Зроблено висновки про структурно-функціональні зв'язки, що визначають залежність циклічності дихання клітини від синхронізації функціонування циклу трикарбонових кислот та електротранспортного ланцюга.